2019 년 2 월

석사학위 논문

ASTRIN mediates RIF1-related DNA damage response

조선대학교 대학원

의과학과

양 은 비

ASTRIN mediates RIF1-related DNA damage response

2019 년 2 월 25 일

조선대학교 대학원

의과학과

양 은 비

ASTRIN mediates RIF1-related DNA damage response

지도교수 이 정 희

이 논문을 이학석사학위신청 논문으로 제출함

2018 년 10 월

조선대학교 대학원

의과학과

양 은 비

양은비의 석사학위논문을 인준함

위원장 조선대학교 교 수 장인엽(인)

위 원 조선대학교 교 수 유호진(인)

위 원 조선대학교 교 수 이정희(인)

2018년 11월

조선대학교 대학원

CONTENTS

RESULTS

CONTENTS OF FIGURES

국문초록

ASTRIN의 DNA 손상 반응 조절 연구

양 은 비

지도교수: 이 정 희

조선대학교 일반대학원

의과학과

DNA 이중나선 절단에 의한 DNA 손상은 주로 비상동말단결합과 상동재조합에 의해 복구된다. RIF1은 비상동말단결합을 촉진하며, NBS1은 상동재조합에 있어서 필수적이다. 이러한 DNA 이중나선 절단 복구의 선택은 DNA 말단절제 유무에 의해 결정된다. 그러나 이런 DNA 말단절제 조절에 대한 자세한 기전은 아직 밝혀지지 않았다. 본 연구에서는 Yeast two-hybrid screening을 통해

DNA 말단절제를 조절하는 중요한 단백질인 RIF1, NBS1과 결합하는 ASTRIN이라는 단백질을 동정하였다. 흥미롭게도, 방사선 조사 후 세포 내에서 ASTRIN과 NBS1의 결합이 증가하고, RIF1과의 결합은 감소됨을 확인하였다. 이는 방사선 조사에 따른 DNA 이중나선 절단 복구에서 ASTRIN의 역할이 기능적으로 다른 두 복구기전에 관여할 수 있음을 시사한다. ASTRIN이 결핍된 세포에서 colony survival assay, late γ-H2AX 염색법 등을 통해 DNA손상 복구 활성이 떨어짐을 확인하였다. 그 다음으로, ASTRIN이 RIF1, NBS1 활성조절에 미치는 영향을 알아보기 위해, ASTRIN이 결핍된 세포에서 방사선 조사 후 RIF1의 DNA손상 foci가 감소되고, NBS1 foci, MRE11 foci, RPA foci, RAD51 foci가 증가되는 것을 각 단백질에 대한 면역염색을 통해 확인하였다. 그러나, 53BP1 손상 foci는 ASTRIN의 존재에 영향을 받지 않았다. 더 나아가, ASTRIN 결손에 의해 비상동말단결합 활성이 저하되고, 상동재결합 활성을 증진시킴을 EJ5-, DR-GFP 벡터 시스템을 통해 확인하였다. ASTRIN이 결손되었을 때, DNA 말단절제술이 증가됨을 G1기에서의 RPA foci와 말단절제술 측정

법을 통해 확인하였다. 마지막으로, 세포 내 ASTRIN의 저하는 적절한 DNA 이중나선 절단 복구를 하지 못하므로 비정상적인 염색체가 증가됨을 metaphase chromosome spreads assay 통해 증명하였다. 따라서, 본 연구는 ASTRIN이 RIF1/NBS1과 결합하여, DNA 말단절제를 조절함으로써 DNA 이중나선 절단에 의한 비상동말단결합/상동재결합을 선택하는데 중요한 조절자임을 제안한다.

INTRODUCTION

DNA double-strand breaks (DSBs) are generated by the action of exogenous agents, such as ionizing radiation or radiomimetic chemicals [1]. The DSBs must be repaired correctly to preserve genomic stability. Indeed, defective DSB repair is associated with various developmental, immunological, and neurological disorders, and is a major driver in cancer [2]. DSBs are repaired mostly by non-homologous end joining (NHEJ) and homologous recombination (HR).

NHEJ, which does not require sequence homology, is active throughout the cell cycle but is particularly important during the G1 phase of the cell cycle [1, 3, 4]. NHEJ promotes direct ligation of the DSB ends, but in an error-prone manner, frequently resulting in small insertions, deletions, substitutions at the break site, and translocations if DSBs from different parts of the genome are joined [2, 3]. RIF1 promotes classical NHEJ over more error-prone alternative end joining in G1 [4-7]. RIF1 is the most proximal effector in anti-resection function [6].

Recently, REV7 identified as a downstream factor in 53BP1-/RIF1-dependent DSB repair pathway choice [6, 8, 9]. REV7 promotes NHEJ by inhibiting 5′ end resection downstream of RIF1 [8]. Shieldin discovered a vertebrate-specific novel protein complex, which functions as a downstream effector of RIF1 in the NHEJ pathway [6]. Shieldin complex is comprised of REV7 plus three previously uncharacterized proteins, RINN1 (CTC-534A2.2), RINN2 (FAM35A), and RINN3 (C20ORF196) [6]. NHEJ was reported that regulated by cascade of 53BP1-RIF1-REV7-Shieldin until now.

HR predominates in the mid-S and mid-G2 cell cycle phases, when the sister template is available [5, 10]. NBS1 is a component of the MRE11/RAD50/NBS1 complex [11-13]. MRN complex binds to DSB ends and promotes end resection to initiate HR. CtIP interacts to NBS1 and recruits at DSB ends. Although CtIP is not nuclease, promotes the nuclease activity of MRN complex and then processes DSB ends [5]. To the next, ExoI nuclease termi-

nates DNA end resection [4, 5]. Once produced, ssDNA is bound by replication protein A (RPA), which is then replaced by the RAD51 protein that promotes DNA strand-invasion and ensuing HR [14, 15].

The first control point for DNA repair pathway choice is the processing of the DNA break [16, 17]. DNA end resection inhibits NHEJ and allows HR [17, 18]. Therefore, DNA end resection is worked more S/G2 than G1. In DNA end, RIF1 inhibits end resection and promotes NHEJ but, NBS1 initiates DNA end resection [4, 5, 19]. The choice between NHEJ and HR depends on the DNA end resection and phase of the cell cycle.

ASTRIN, also known as SPAG5, has been shown to spindle-associated protein [20]. In addition, depletion of ASTRIN induces a p53-dependent apoptosis [21]. The association of ASTRIN at the centrosome requires hNinein during the S phase and G2 phase of the cell cycle [22]. ASTRIN and Snm1B act in a common pathway to effect the prophase checkpoint [23]. Currently, ASTRIN is in-

volved in cell proliferation and apoptosis via upregulating Wnt3 by activating the AKT/mTOR signaling pathway [24]. ASTRIN is a nonmotor coiled-coil domain containing protein in its C-terminal [20-22, 25]. Although ASTRIN was reported on relation of mitosis and apoptosis, its function remains unknown in DNA damage response.

In this study, we identified ASTRIN as binding partner of RIF1 and NBS1 through yeast two hybrid screening. We confirmed interaction between ASTRIN and RIF1/NBS1 by proximity ligation assay (PLA) and co-immunoprecipitation (IP) assay. Also, depletion of ASTRIN results in cellular hypersensitivity and impaired DNA damage repair to IR, as detected by colony survival assay and late γ-H2AX foci staining. Moreover, we showed a various DNA damage foci in ASTRIN absence or presence condition. We showed that ASTRIN-depleted cells impaired non-homologous end joining repair and enhanced homologous recombination. Furthermore, knockdown of ASTRIN results in increase of RPA damage

foci and DNA end resection after ionizing radiation (IR). Finally, in absence of ASTRIN, an increase of chromosome instability showed by metaphase chromosome spreads assay. Thus, we propose that ASTRIN function as a regulator of DNA end resection is critical for choice of DNA double strand break repair.

MATERIALS AND METHODS

1. Cell culture and treatment of ionizing radiation

HeLa and U2OS cells were purchased from ATCC. They were cultured in Dulbecco's modified Eagles's medium (DMEM) supplemented with 10% fetal bovine serum and streptomycin (0.1 mg/ml), penicillin (100 units/ml) at 37 ℃ in a 5% CO_2 incubator. Cell growth was monitored under an inverted microscope. Upon reaching 70-80% confluency, cells were digested with 1 x trypsin-EDTA before being passaged. Cells in exponential growth were harvested for subse-quent experiments. To induce DNA double strand breaks, exponentially growing cells were irradiated at 5 Gy from ^{137}Cs source (Gamma cell 3000 Elan irradiator, Best Theratronics) and allowed to recover at 37 ℃ incubator for various times.

2. siRNA transfection

HeLa and U2OS cells were transfected with siRNA oligonucleotide duplexes against ASTRIN using RNA IMAX (Invitrogen) according to the manufacture's instruction. The siRNA sequences targeting ASTRIN (ASTRIN siRNA #1: 5′-GGCCCGTTTAGATACCATG-3′, ASTRIN siRNA #2: 5′-CCATGCAACTGGATTATACAA-3′, ASTRIN siRNA #3: 5′-CCAAATTAGCTCTACTCCTAA-3′, ASTRIN siRNA #4: 5′-GAGTTTGCAGACCAGGAGAAT-3′, ASTRIN siRNA #5: 5′-CGCTCTGACAAGGAGTTAGAA-3′), siRIF1 (RIF1 siRNA: 5′-GACTCACATTTCCAGTCAA-3′), siBRCA1 (BRCA1 siRNA: 5′-TCACAGTGTCCTTTATGTA-3′), siRAD51 (RAD51 siRNA: 5′-CTAATCAGGTGGTAGCTCATT-3′) designed and synthesized for transient transfection.

3. co-Immunoprecipitation assay

The whole cell lysates prepared by extracting with RIPA buffer (50 mM Tris (pH 7.5), 1% Triton X-100, 150 mM Sodium Chloride, 2 mM EDTA, 0.5% Sodium deoxycholate and 0.1% SDS) with protease inhibitors (Roche Diagnostic Corp.). The lysates were added to anti-ASTRIN antibody (Proteintech) at 4 ℃ overnight. And then, G-sepharose (GE Healthcare) was added to the lysates, and beads mixtures were incubated at RT for 1 hour with shaking. The beads were washed four times in RIPA buffer without protease inhibitors, resuspended in equal volume 2 x SDS sample buffer. The samples were extracted from the bead by boiling at 100 ℃ for 5 min. The samples were then analyzed by western blotting using the appropriate antibodies.

4. Western blot analysis

Cells were lysised in RIPA buffer (50 mM Tris (pH 7.5), 150 mM NaCl, 1% NP-40, 0.5% sodium deoxycholate (NADOC), 0.1% sodium dodecyl sulfate (SDS)) with protease inhibitors (Roche Diagnostic Corp.). Cell lysates were collected by centrifugation at 15,000 rpm for 30 min. Protein concentrations were measured using the Bradford assay (Bio-Rad). Equal amounts of protein were separated by 6-15% SDS-PAGE followed by electro transfer onto a polyvinylidene difluoride membrane (Millipore, Bedford, MA, USA). The membranes were blocked for 1 hour with TBS-t (10 mM Tris (pH 7.4), 150 mM NaCl and 0.1% Tween-20) containing 5% skim milk and then incubated at 4 ℃ with primary antibodies (1:1000) overnight. The blots were washed six times for 10 min with 0.1% Tween-20 containing TBS-t and then incubated for 2 hours with peroxidase-conjugated secondary antibodies (1:4000) at RT. The membranes were washed six times for 10 min, and developed using an enhanced chemilumines-

cence detection system (ECL; GE Healthcare, Buckinghamshire, UK).

5. Antibodies

We used the following primary antibodies: Rabbit polyclonal anti-SPAG5 (14726-1-AP, Proteintech), Rabbit polyclonal anti-RIF1 (A300-567A, Bethyl), Mouse monoclonal anti-NBS1 (611870, BD), Rabbit polyclonal anti-NBS1 (A301-284A, Bethyl), Goat polyclonal anti-Nibrin (sc-8580, Santa Cruz), Mouse monoclonal anti-HA (sc-7392, Santa Cruz), Rabbit monoclonal anti-HA (3724S, Cell Signaling), Rabbit polyclonal anti-HA (NB600-363, Novus), Mouse monoclonal anti-ß-actin (sc-47778, Santa Cruz), Rabbit polyclonal anti-CENP/F antibody (ab5, Abcam) , Mouse monoclonal anti-53BP1 (612523, BD), Rabbit polyclonal anti-MRE11 (NB100-142, Novus), Mouse monoclonal anti-RPA (2772534, Calbiochem), Rabbit polyclonal anti-RAD51 (sc-8349, Santa Cruze) and Mouse monoclonal anti- γ -H2AX(05-636, Millpore).

6. In situ proximity ligation assay (PLA)

The primary antibodies need to be optimized through concentration titration to make sure that they work properly before the star of proximity ligation assay, and IgG from the same isotype and species was usually used as negative control. The cells were transferred on the coverslip in plates and grown to 50-70% confluency. The cells were washed with PBS, fixed with 4% formaldehyde for 15 min, permeabilized with 0.1% Triton X-100 for 10 min, washed, and then blocked using Duolink blocking buffer for 1 hour. The coverslips were transferred into a humidified chamber and then a small volume of primary antibodies targeting the proteins under investigation were pipetted onto each coverslip. Atigen-antibody interaction will mostly accomplish overnight at 4 ℃ with gentle agitation. The two corresponding PLA probes were mixed and diluted in the antibody diluent. Allow the mixture to sit for 20 min at RT. The samples were washed with 0.05% Tween-20 containing PBS twice, and then incubated with

PLA probes MINUS and PLUS (DUO92005, Sigma) for 1 hour at 37 ℃. The samples were washed in 1 x wash buffer A (0.01 M Tris, 0.15 M NaCl, 0.05% Tween-20, pH 7.4) for 5 min twice under gentle agitation, and the probes were ligated with two other circle-forming DNA oligonucleotides by ligation-ligase solution for 30 min at 37 ℃. The samples were washed in 1 x wash buffer A for 2 min twice under gentle agitation and two added oligonucleotides by enzymatic ligation were amplified via rolling circle amplification by the incubation with am-plification-polymerase solution over 90 min at 37 ℃. The samples were washed in 1 x wash buffer B (0.2 M Tris, 0.1 M NaCl, pH 7.5) for 10 min twice followed by 0.01 x wash buffer B for 1 min by diluting 1 x buffer B (1:1000) in high purity water. The samples were dried in hood for approximately 10 min at RT in the dark, the cells were mounted using Vectashield mounting medium with 4, 6-diamidino-2-phenylindole (Vector Laboratories, Burlingame, CA, USA). Fluo-rescence images were taken using a confocal microscopy (Zeiss LSM510 Meta:

Carl Zeiss) analyzed with ZEN software

7. Plasmids

The full length ASTRIN cDNA was amplified from HeLa cell by RT-PCR using the ASTRIN primers 5′-CTC GAG ATG TGG CGA CTG AAA A-3′ (sense) and 5′-GGG CCC TTA GCT CAG AAA TTC CAG CAA-3′ (antisense). The amplified ASTRIN cDNA construct was cloned into the mammalian expression vector pcDNA3 in frame with the hemagglutinin (HA) tag and using the primers (a.a 1-608) 5′-CTC GAG ATG TGG CGA CTG AAA A-3′ (sense) and 5′-GGG CCC TTA TTC CCG CAT GGA TGC TA-5′ (antisense), (a.a 609-1193) 5′-CTC GAG TTC AGA GGC CTT CTG AAG GAT-3′ (antisense).

8. Colony survival assay

After treatment with IR, $1x10^3$ cells were immediately seeded onto a 60 mm dish in duplicate and grown for 2-3 weeks at 37 ℃ to allow colony formation.

Colonies were fixed with 100% methanol for 10 min and stained with 1% Methyleneblue in 20% Ethanol and counted. The fraction of surviving cells was calculated as the ratio of the plating efficiencies of treated cells to untreated cells.

9. Immunofluorescence microscopy

To visualize nuclear foci, cells were grown on glass coverslips and were irradiated with 5 Gy of ionizing radiation (IR). Cells were then washed twice with 0.01 M PBS, fixed with 4% paraformaldehyde for 15 min and 100% methanol for 5 min, followed by permeabilization with 0.5% Triton X-100 for 15 min at RT. Next, the cover slips were washed three times with 0.01 M PBS and then blocked with 5% BSA in 0.01 M PBS for 1 hour. The cells were immunostained with primary antibodies against various proteins overnight at 4 ℃. Next, the cells were washed with 0.01 M PBS and then stained with Alexa Fluor 488 (green, Molecular Probes) or Alexa Fluor 594 (red, Molecular Probes) conjugated secondary antibodies, as appropriate. After washing, the cells were

mounted using Vectashield mounting medium with 4, 6-diamidino-2-phenylindole (Vector Laboratories, Burlingame, CA, USA). Fluorescence images were taken using a confocal microscopy (Zeiss LSM510 Meta: Carl Zeiss) analyzed with ZEN software.

10. Non-homologous end joining assay

To measure the NHEJ repair, stable cells lines expressing HeLa EJ5-GFP report were generated by transfection using turbofectamine. EJ5-GFP contains a promoter that is separated from a GFP coding region by puromycin resistance gene, which is flanked by two I-SecI sites that are in the same orientation. When the I-SecI-induced DSBs are repaired by NHEJ in HeLa EJ5-GFP cells, the puro gene is removed, and the promoter is rejoined to the rest of the GFP expression cassette, leading GFP expression. EJ5-GFP cells were transfected with control siRNA, ASTRIN siRNA, RIF1 siRNA, and BRCA1 siRNA after 5 hours transfected with 0.5 ug of I-SceI-expressing vector and HA vector or HA-

ASTRIN full length. After 43 hours, the cells fixed 4% paraformaldehyde and stained 5 ug/ml Hoechst (Sigma) for 1 hour. The images were shown at x20 magnification using an IN Cell Analyzer 2500 HS (GE Healthcare)

11. Homologous recombination assay

To measure the HR repair, stable cell lines expressing U2OS DR-GFP report were generated by transfection using turbofectamine. DR-GFP is shown along with the HDR product that uses *iGFP* as the template for nascent DNA synthesis, which results in restoration of a GFP expression cassette. DR-GFP cells were transfected with control siRNA, ASTRIN siRNA, RIF1 siRNA, and RAD51 siRNA after 5 hours transfected with 0.5 ug of I-SceI-expressing vector and HA vector or HA-ASTRIN full length. After 48 hours, the cells fixed 4% paraformaldehyde and stained 5 ug/ml Hoechst (Sigma) for 1 hour. The images were shown at x20 magnification using an IN Cell Analyzer 2500 HS (GE Healthcare).

12. 5′ end resection assay

In vivo DNA 5′ end resection was measured in AID-DIvA U2OS cells. The target proteins were knocked down by siRNA. After 48 hours, AsiSI-mediated DSBs were induced by treating the cells with 4-OHT for 4 hours. Genomic DNA was isolated using Genomic DNA Extraction Kit (BIONEER). 3 ug of RNaseH treated genomic DNA was digested overnight with BamHI and HindIII digestion at 37 ℃. To quantify the extent of resection, the availability of selected DNA sites were measured by qPCR using 18 ng of restriction enzyme digested or un-digested genomic DNA using specific Taqman probes. The ssDNA percent was calculated from the change in Ct values of mock and restriction enzyme digested DNA using the following equation: ssDNA% = 1/(2^(⊿Ct-1)+0.5)*100. At least three biological repeats were performed and data are presented as the mean ± SEM [26].

13. Metaphase chromosome spreads assay

Grow cells were added colcemid (Sigma) 100 ng/ml for 3 hours and then were incubated at 37 ℃ overnight. After incubation, the medium were transferred to a 15 ml tube. The plate was washed with 1 x Trypsin-EDTA and was transferred to the tube and incubated at 37 ℃ for 5 min. The cells were collected by centrifugation at 1,000 rpm for 5 min and were resuspended by the medium. KCl solution was slowly added and was incubated at RT for 30 min. The cells were collected by centrifugation at 1,000 rpm for 10 min and were resuspended by the medium. Cold Carnoy's fixative was slowly added and was incubated at RT for 10 min. The cells were collected by centrifugation at 1,000 rpm for 10 min. Repeat step (Fixation) 3 additional time. The supernatants were aspirated as much as possible. The cell's volume was resuspended by small volume of fixative, until the cell suspension look slightly milky. Slides were soaked acetic acid overnight, were rinsed in running water for 10 min and then were

rinsed in absolute ethanol, air-dry it. Slides were put at -20 ℃ until use. Misten it by breathing and drop 100 ul fixed cells onto glass slides. Glass slides were dried at RT overnight. The cells were mounted using 4, 6-diamidino-2-phenylindole (Vector Laboratories, Burlingame, CA, USA). Fluorescence images were take using a confocal microscopy (Zeiss LSM510 Meta: Carl Zeiss) analyzed with ZEN software.

14. Statistical analysis

Data in all of the experiments are presented as the mean ± standard deviation (SD). Analyses were performed using software (Image J) and Excel (Microsoft).

RESULT

1. ASTRIN interacts with RIF1 and NBS1.

The DNA end resection is the vital factor in the double strand break (DSB) repair pathway choice. RIF1 inhibits and NBS1 promotes DNA end resection. But, its regulation and underlying mechanism are only partially understood. In order to better characterize the DNA end resection regulatory network relevant to RIF1 and NBS1, a yeast two-hybrid screen was performed. The common clone of RIF1 and NBS1 isolated from these transformants was identified as human ASTRIN. A mitotic-associated protein, ASTRIN, was identified as a novel binding partner for RIF1 and NBS1.

To confirm the binding between ASTRIN and RIF1/NBS1, we performed Proximity Ligation Assay (PLA) staining that detects protein-protein interaction. HeLa cells were treated with 5 Gy ionizing radiation (IR) for 3 hours and were then fixed. The cells were each other stained with an anti-RIF1 antibody and an

anti-NBS1 antibody. ASTRIN was ligated to PLA probes MINUS and PLUS. Normal rabbit IgG was used as negative control of PLA staining. The red dots indicated interaction between RIF1/NBS1 and ASTRIN (Figure 1A and 1B).

In the result of PLA, the red dots were different quantification in accordance with irradiation condition. To look for this interaction in vivo, co-immunoprecipitation (IP) assay and western blotting was performed using the anti-ASTRIN, anti-RIF1, and anti-NBS1 antibodies. The Rabbit IgG was used as negative control of co-IP assay. As shown in Figure 1C, endogenous RIF1/NBS1 and ASTRIN co-immunoprecipitated from cell extracts. Interestingly, NBS1 increased binding to ASTRIN (2-folds) and RIF1 decreased binding to ASTRIN (3-folds) after IR (Figure 1D). These results suggest that ASTRIN interacts with RIF1 and NBS1 each other and may play a role in DNA damage response (DDR).

Figure 1

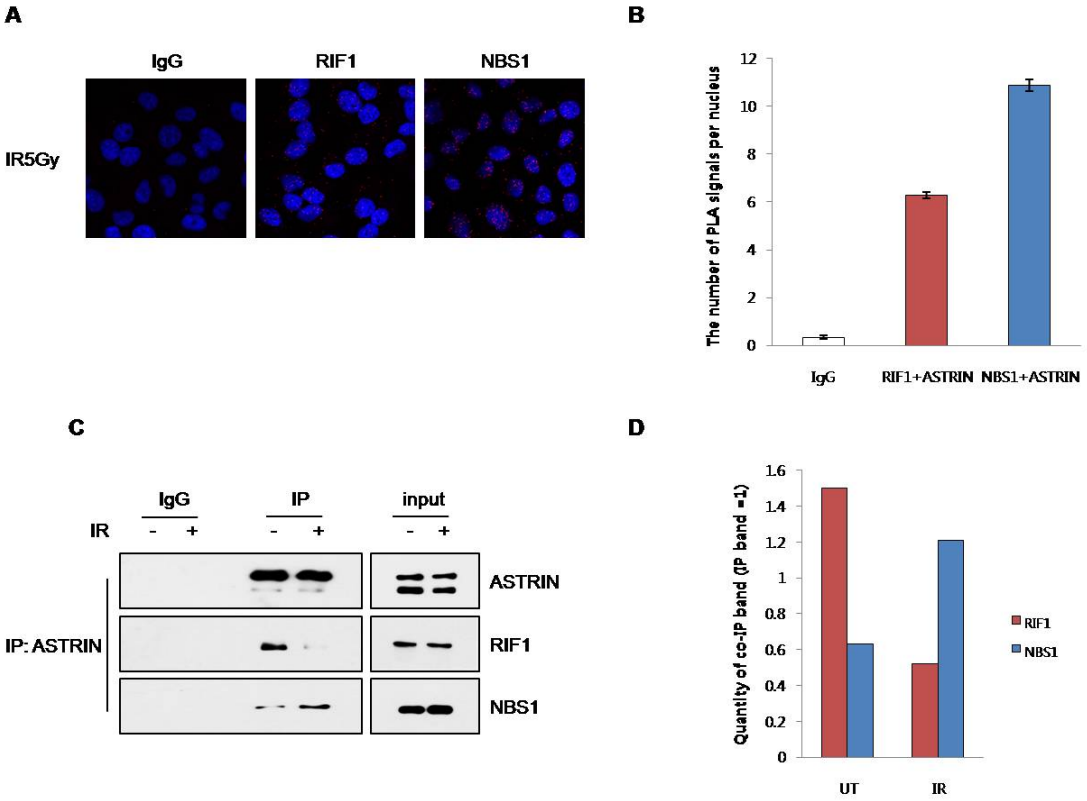

Figure 1. ASTRIN binds differently RIF1 and NBS1 according to IR treatment.

(A) Control- and ASTRIN-depleted HeLa cells were treated with 5 Gy IR for 3 hours and were then fixed. The cells were each other stained with the anti-RIF1 antibody and anti-NBS1 antibodies. ASTRIN was ligated through PLA probes MINUS and PLUS. **(B)** Quantification of PLA signal. **(C)** HeLa cells were un-treated or treated with 5 Gy IR for 3 hours. Whole cell lysates were subjected to IP using an anti-ASTRIN antibody followed by Western blotting using the anti-ASTRIN, RIF1 and NBS1 antibodies. **(D)** The intensity of RIF1 and NBS1 bands was normalized to that of the ASTRIN band using Image J software. Results are shown as mean ±SD (n=3).

2. The N-term domain of ASTRIN is critical for interaction of RIF1 and NBS1.

To further confirm the binding site of ASTRIN, we have generated the constructs encoding HA-FL (1-1193 a.a, 131kDa), N-terminal (1-608 a.a, 66kDa), and C-turminal (609-1193 a.a. 64kDa) mutants of ASTRIN (Figure 2A). As shown in Figure 2B, after HeLa transfected with constructures, the HA-tagged ASTRIN expression from each construct was analyzed by Western blotting with an anti-HA antibody. The β-actin was used as loading control.

Next, the interaction between these proteins was also confirmed by co-IP and western blotting of overexpressed HA-tagged ASTRIN constructs. We found that the N-terminal pro-rich domain of ASTRIN is responsible for their interaction (Figure 2C). Through above results, we indentified the N-terminal pro-rich region as important for interaction of RIF1 and NBS1.

Figure 2

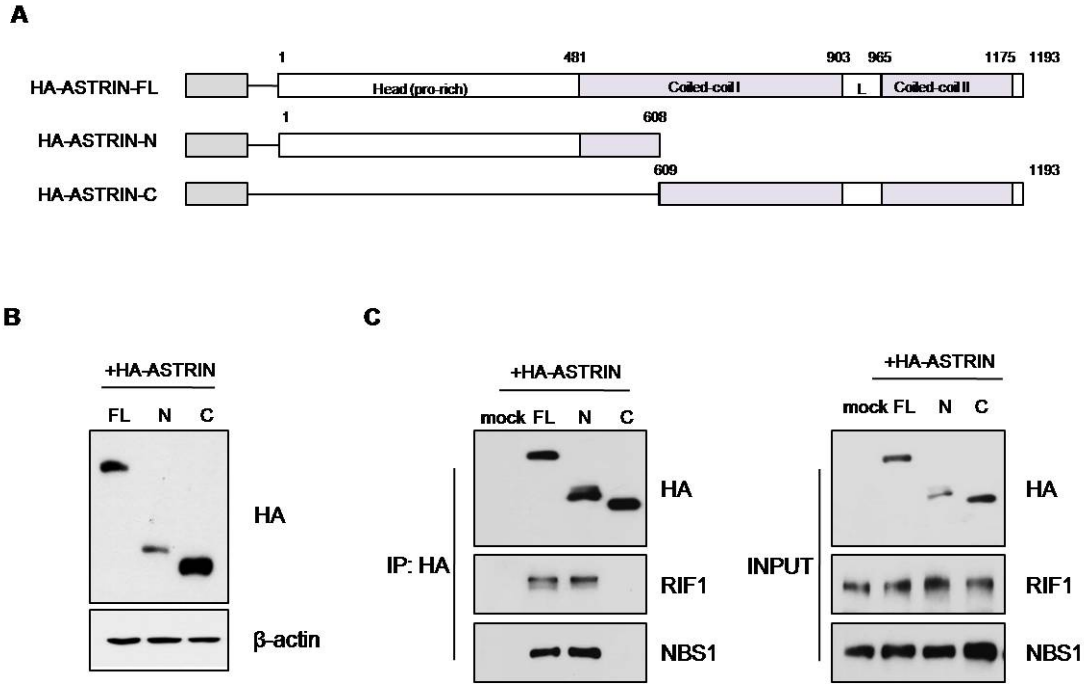

Figure 2. The N-terminal of ASTRIN is required for RIF1 and NBS1 interaction.

(A) Schematic representation of three HA-tagged ASTRIN constructs. HA-tagged full length ASTRIN (HA-ASTRIN-FL, 1-1193 a.a), HA-tagged N-terminal (1-608 a.a) mutant of ASTRIN (HA-ASTRIN-N), and HA-tagged C-terminal (609-1193 a.a) mutant of ASTRIN (HA-ASTRIN-C). **(B)** HeLa cells were transiently transfected with each constructs. After 48hours, HeLa cells were harvested and analyzed by Western blotting. **(C)** HeLa cells were prepared as in Figure 2B, and the cell lysates were subjected to IP using an anti-HA antibody followed by Western blotting using the anti-HA, RIF1 and NBS1 antibodies.

3. Knockdown of ASTRIN is hypersensitive to ionizing radiation.

The association between ASTRIN and RIF1/NBS1 suggested the involvement of ASTRIN in the DSB repair. First, we designed five type of siRNA against ASTRIN, recognizes CDS sequence of ASTRIN-mRNA. We named these siRNA to siASTRIN #1, siASTRIN #2, siASTRIN #3, siASTRIN #4, and siASTRIN #5, respectively (Figure 3A). To check how efficient this siRNA interfered expression of ASTRIN gene, we performed western blot assay using an anti-ASTRIN antibody. The β-actin was used as loading control (Figure 3B). All of ASTRIN siRNA work efficiently, we used siASTRIN #3 to next experiment.

To investigate the potential role of in DDR, we hypothesize ASTRIN-depleted cells would be more sensitive to DNA damage. Control and ASTRIN siRNA transfected HeLa cells were treated with indicated does of IR, and then monitored for 14 days. We found that ASTRIN-depleted cells exhibited reduction of colony numbers after treatment with IR, compared to control cells (Figure 3C and 3D). Therefore, we considered ASTRIN as DDR regulator.

Next, IR-induced γ-H2AX foci was stained an anti-γ-H2AX antibody and analyzed by immunofluorescence microscopy. As DNA damage marker, γ-H2AX is used as the indicator for DNA repair. γ-H2AX foci formation is suggested that the cells with unrepaired DNA damage still remain. Control cells rapidly formed γ-H2AX foci following exposure to IR, and these focus were almost completely resolved 24 hours after the exposure, indicating efficient DNA repair. ASTRIN-depleted cells also rapidly formed γ-H2AX foci after irradiation exposure, but 24 hours later, large amount of foci still remained (Figure 3E and 3F). These results suggest that ASTRIN promotes DSB repair.

Figure 3

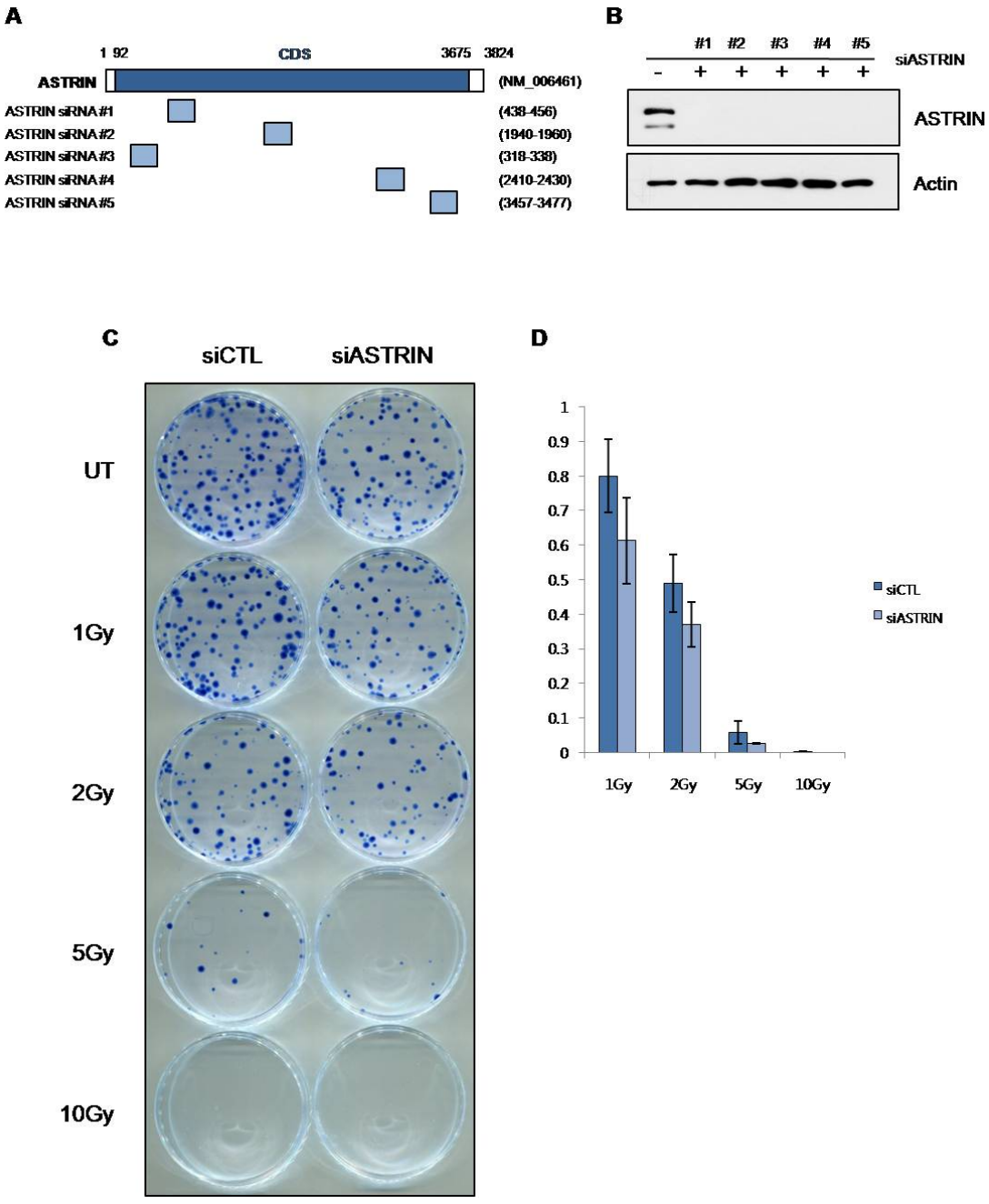

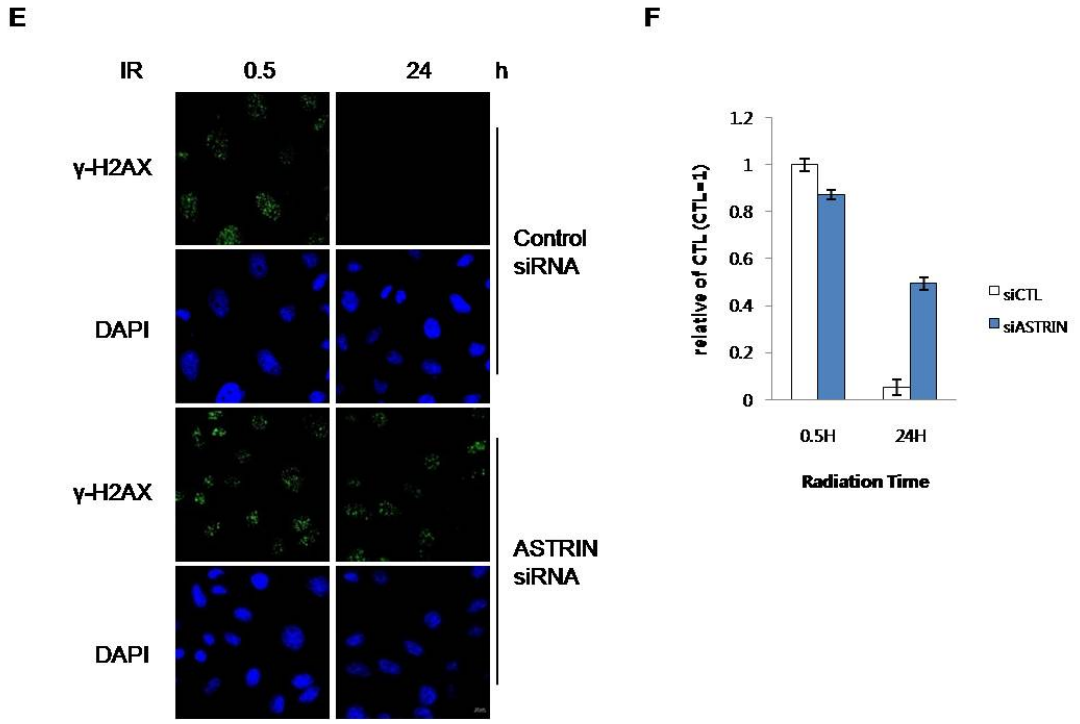

Figure 3. ASTRIN-depleted cells are hypersensitive to IR.

(A) Schematic diagram of human ASTRIN siRNA sequences. The position of CDS (dark blue), we designed ASTRIN #1, 2, 3, 4, and 5 siRNA (light blue). (B) HeLa cells were transfected with control, ASTRIN #1, 2, 3, 4, and 5 siRNA. After 48 hours, the expression level of ASTRIN was confirmed by western blotting using an anti-ASTRIN antibody. (C) ASTRIN affects sensitivity of cells following exposure to IR in HeLa cells. Control- and ASTRIN-depleted HeLa cells were untreated or treated with 1, 2, 5 and 10 Gy IR. After 2 weeks, cells were stained with methylene blue, and the number of surviving colonies was counted. (D) Quantification of Figure 3C. (E) Control- and ASTRIN-depleted HeLa cells were untreated or treated with 5 Gy IR and were then fixed at the indicated times. The cells were stained with an anti-γ-H2AX antibody and the nuclei were counterstained using DAPI. (F) Quantification of Figure 3E. The histogram shows the number of cells with foci. Results are shown as mean $\pm$SD (n=3).

4. ASTRIN upregulates RIF1 foci formation after ionizing radiation.

Because ASTRIN may be DDR regulator and interacts with RIF1, we wondered RIF1 foci formation in depletion of ASTRIN. Control- and ASTRIN-depleted cells were treated with 5 Gy IR to make DSBs and harvested in different time intervals. The cells were fixed and immunofluorescence assay performed. The knockdown of ASTRIN cells had significantly fewer RIF1 foci following IR exposure than control cells (Figure 4A and 4B).

53BP1 also has been reported RIF1-related DNA damage repair. Next, we questioned whether the ASTRIN affect 53BP1 foci formation following IR treatment. To test this possibility, we were performed immunostained with an anti-53BP1 antibody after IR treatment. However, transfection of ASTRIN siRNA did not affect 53BP1 foci formation (Figure 4C and 4D). Together, we suggest that ASTRIN is required for RIF1 localization but not affect 53BP1 recruitment at DSBs.

Figure 4

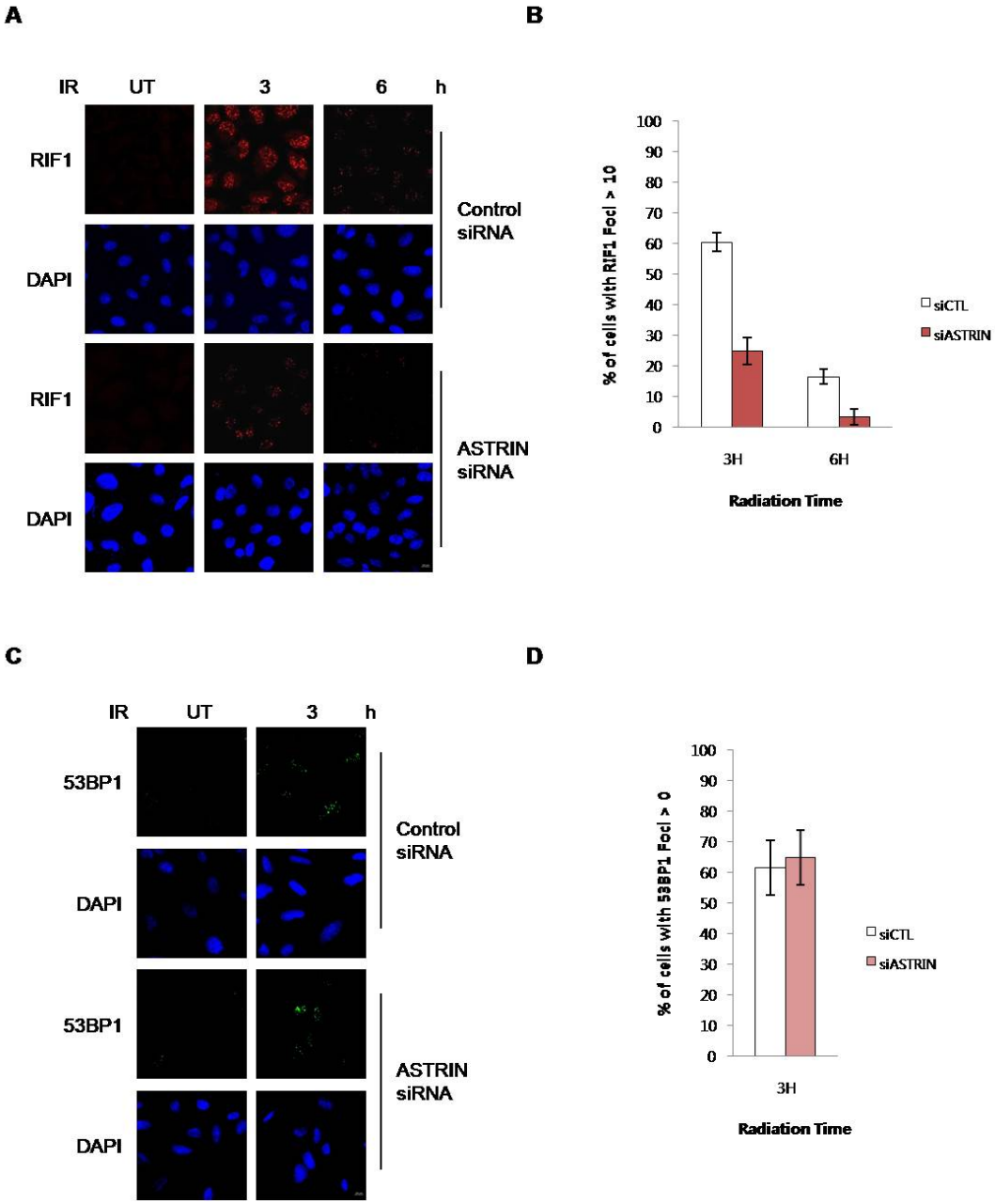

Figure 4. Depletion of ASTRIN decreases RIF1 foci formation to IR.

Control- and ASTRIN- depleted HeLa cells were untreated or treated with 5 Gy IR and were then fixed at the indicated times. (A) The cells were stained with an anti-RIF1 antibody and nuclei were stained with DAPI. (B) Quantification of RIF1 foci > 10 in control- and ASTRIN- depleted cells. (C) The cells were stained with an anti-53BP1 antibody and nuclei were stained with DAPI. (D) Quantification of cells with 53BP1 foci in nuclei. The histogram shows the num-ber of cells with foci. Results are shown as mean ±SD (n=3).

5. ASTRIN promotes Non-homologous end joining.

DNA DSBs can be repaired through NHEJ or HR. Because we showed ASTRIN promoted DSB repair, the next step was to look more closely at two pathways. To measure the involvement of ASTRIN in Non-homologous end joining (NHEJ) mediated repair, we used EJ5-GFP cells, which contain a promoter that is separated from a *GFP* coding cassette by a *puro* gene that is flanked by two I-SceI sites that are in the same orientation (Figure 5A). Once the *puro* gene is excised by NHEJ repair of the two I-SceI induced DSBs, the promoter is joined to the rest of the expression cassette, leading to restoration of the *GFP*+ gene. Since the two I-SceI induced DSBs have complementary 3′ overhangs, such NHEJ could potentially restore an I-SceI site. Alternatively, NHEJ could fail to restore the I-SceI site, leading to an I-SceI resistant site. In addition, a restored I-SceI site could also be re-cleaved and repaired to result in an I-SceI resistant site [27]. We found that an ASTRIN knockdown led to decreased NHEJ

at 67%, and these effects were rescued by ASTRIN cDNA overexpression. Whereas depletion of BRCA1 did not decrease NHEJ, depletion of RIF1 caused reduction of NHEJ (Figure 5B and 5C). These finding indicate that ASTRIN promotes NHEJ by upregulating RIF1.

Figure 5

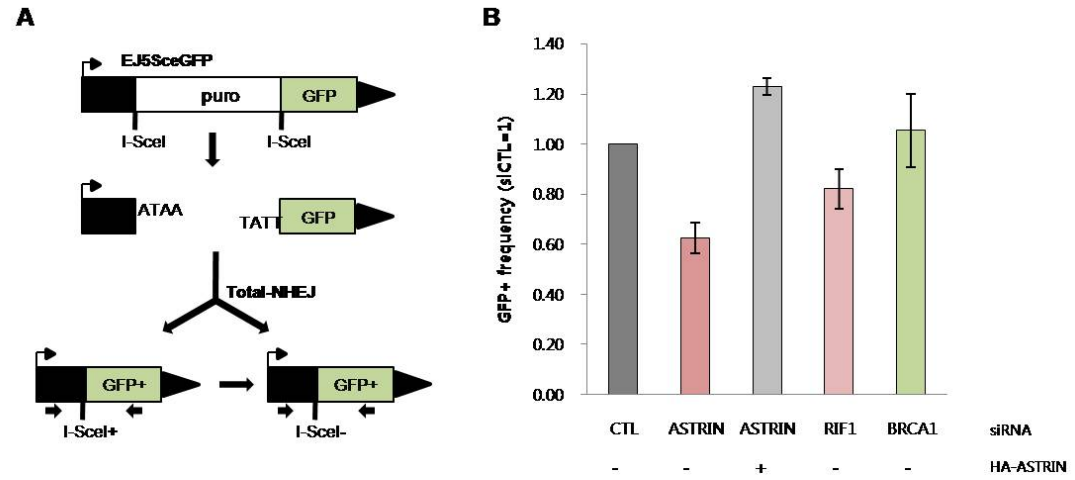

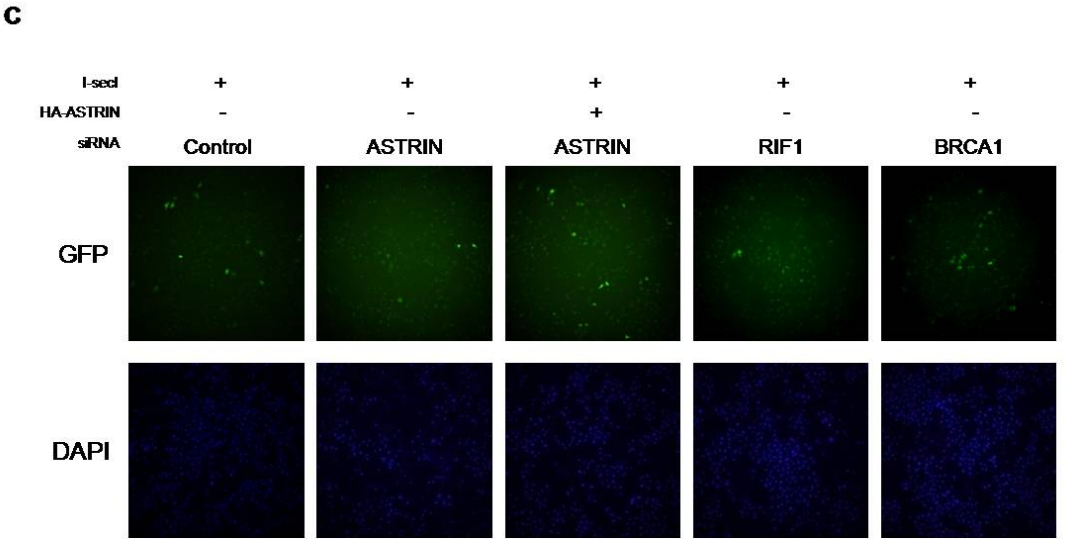

Figure 5. ASTRIN deficiency impairs NHEJ.

(A) A diagram for the NHEJ assay based on the EJ5-GFP reporter, which contains two tandem endonuclease cut sites for the I-SceI. EJ5-GFP contains a promoter that is separated from a GFP coding cassette by a puro gene that is flanked by two I-SceI sites in the same orientation. Once the puromycin gene is excised by the two I-SceI induced DSBs, the promoter is joined to the rest of the expression cassette by NHEJ repair, leading to restoration of the GFP+ gene. (B), (C) HeLa EJ5-GFP cells were transfected with control, ASTRIN, RIF1 and BRCA1 siRNA for 5 hours and then transfected with an I-SceI expression vector and HA vector or HA-ASTRIN full length. After 43 hours, the population of the GFP-positive cells was measured by IN Cell Analyzer 2500 HS. Quantification of cells with GFP expression in control, ASTRIN, RIF1, and BRCA1 siRNA transfected cells. The percentage of GFP expressing cells determined. Results are shown as means ±SD (n=3).

6. ASTRIN downregulates NBS1 foci formation at DSBs.

Because ASTRIN also bind to NBS1, we investigated whether ASTRIN effects IR-induced NBS1 foci formation. Control- and ASTRIN-depleted cells were treated with 5 Gy IR to make DSB and harvested in different time intervals. The cells were fixed and immunofluorescence assay performed. In the absence of ASTRIN, cells with NBS1 foci > 5 were significantly more increase than control cells (Figure 6A and 6B). NBS1 is a component of the MRN complex and MRE11 is important to DNA end resection. So, we confirmed MRE11 foci formation in ASTRIN-depleted cells. MRE11 foci formation was also increased by more than 170% in depletion of ASTRIN (Figure 6C and 6D).

Previously reported RPA had been initially coated single strand DNA (ssDNA) [1]. So, we performed RPA foci formation in ASTRIN-depleted cells. RPA foci formation was also higher than control cells by more than 170% (Figure 6E and 6F). RAD51 had been reported to form a nucleofilament that is essential for ho-

mology searching and the subsequent steps of the HR process [4]. RAD51 foci formation of ASTRIN depleted cells was more increasing than control cells (Figure 6G and 6H). These results suggest that ASTRIN function is downregulator of NBS1 and HR-associated protein foci formation at DSBs.

Figure 6

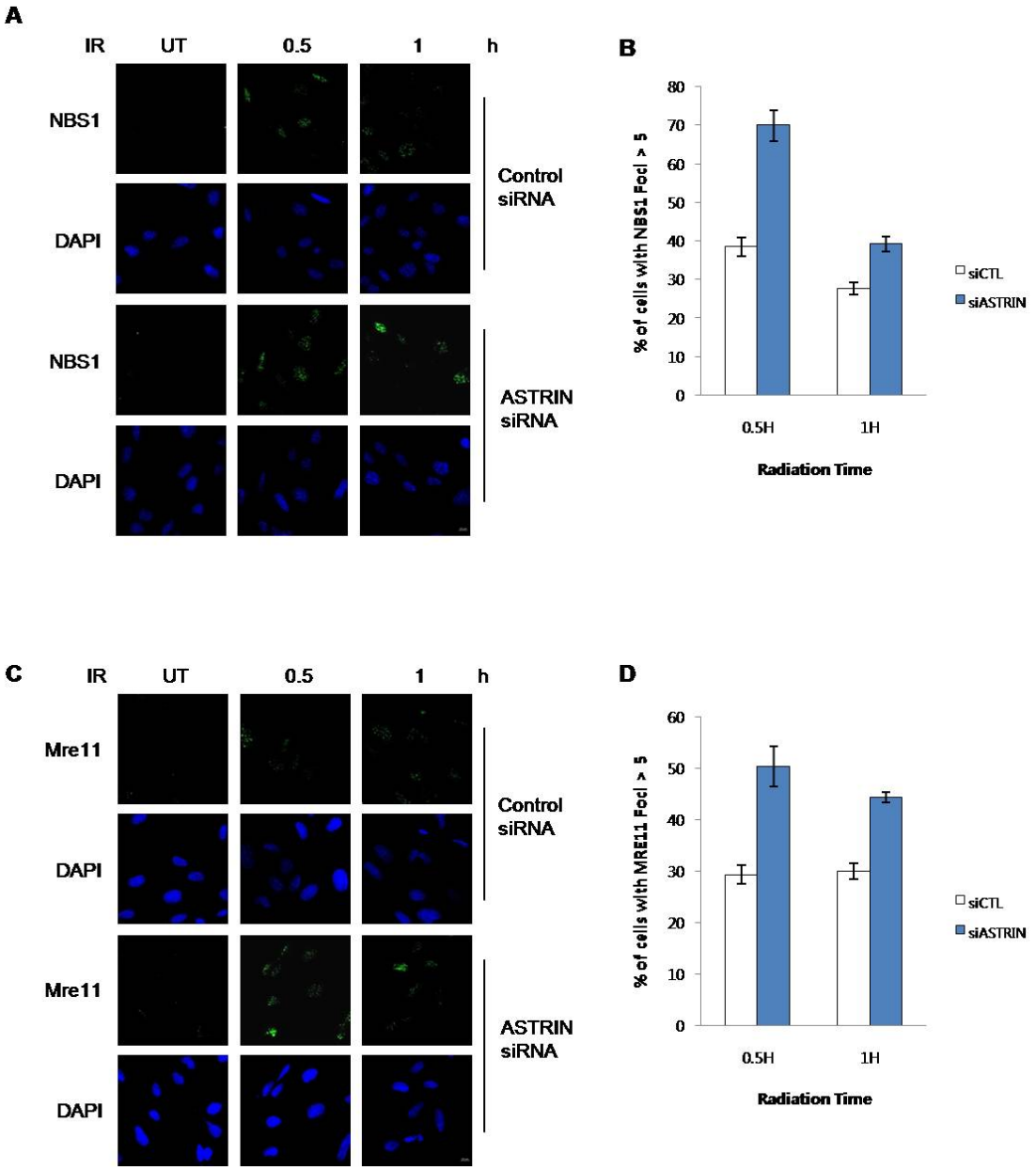

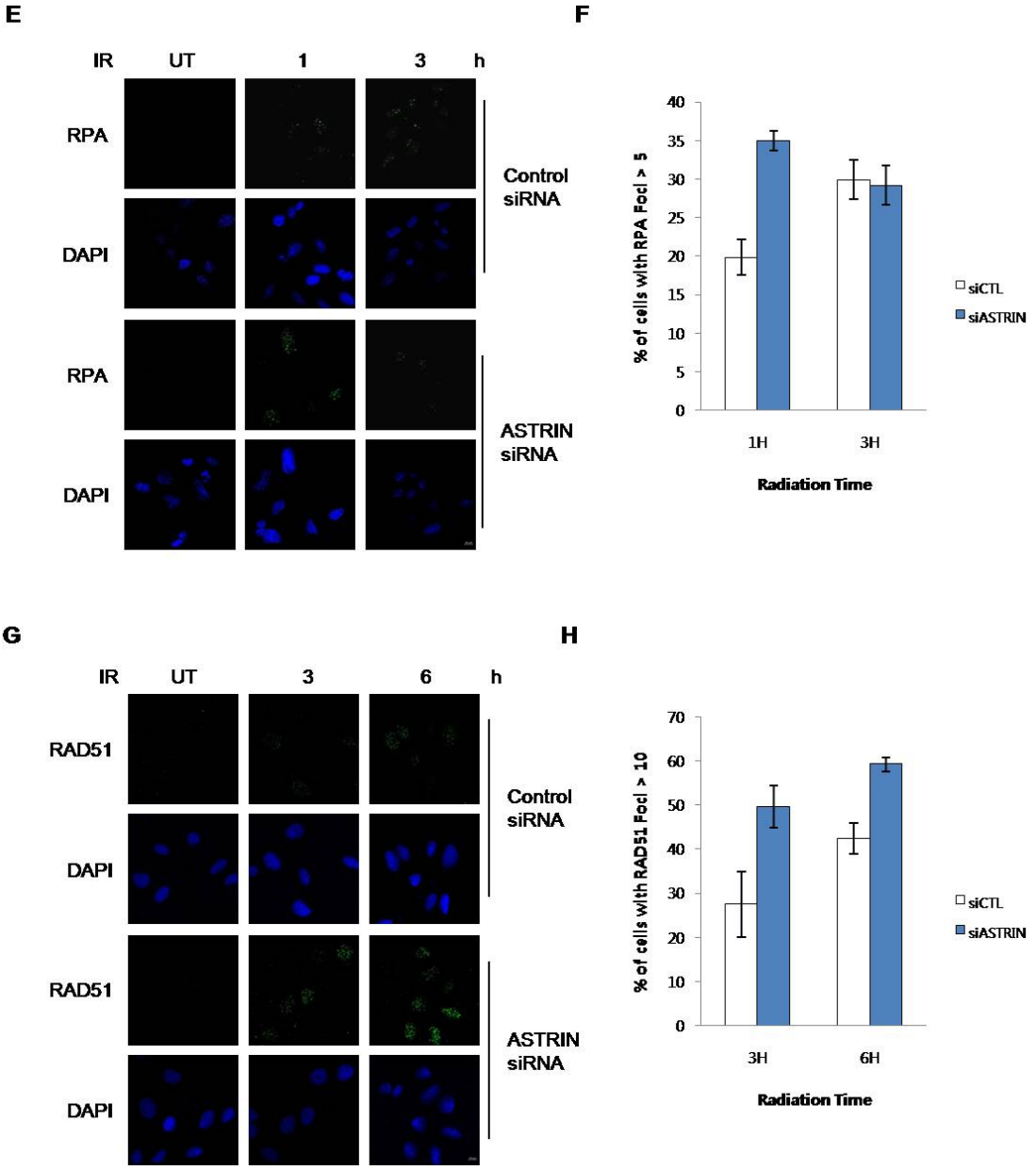

Figure 6. ASTRIN-depleted cells enhance NBS1 and HR related protein foci formation at DSBs.

Control- and ASTRIN-depleted U2OS cells were untreated or treated with 5 Gy IR and were then fixed at the indicated times. **(A)** The cells were stained with an anti-NBS1 antibody and nuclei were stained with DAPI. **(B)** Quantifiaction of NBS1 foci > 5 in control- and ASTRIN- depleted cells. **(C)** The cells were stained with an anti-MRE11 antibody and nuclei were stained with DAPI. **(D)** Quantifiaction of MRE11 foci > 5 in control- and ASTRIN- depleted cells. **(E)** The cells were stained with an anti-RPA antibody and nuclei were stained with DAPI. **(F)** Quantifiaction of RPA foci > 5 in control- and ASTRIN- depleted cells. **(G)** The cells were stained with an anti-RAD51 antibody and nuclei were stained with DAPI. **(G)** Quantifiaction of RAD51 foci > 10 in control- and ASTRIN-depleted cells. The histogram shows the number of cells with foci. Results are shown as mean ±SD (n=3).

7. ASTRIN impairs Homologous recombination.

To demonstrate the role of ASTRIN in the Homologous recombination (HR), we performed HDR assay (Figure 7A). In the DR-GFP reporter strain, DSBs are generated through the expression of I-SecI endonuclease, which cleaves a specific recognition site located in the GFP gene. In this system, repair efficiency via HR is monitored by measuring the percentage of cells expressing GFP. Notably, we found than the knockdown of ASTRIN was more 1.7-fold increase HR than control cells. ASTRIN-induced HR activity was rescued by ASTRIN cDNA overexpression. As positive control, HR was increased by depletion of RIF1 and decreased by depletion of RAD51 (Figure 7B and 7C). Taken together, ASTRIN inhibits homologous recombination by downregulating NBS1.

Figure 7

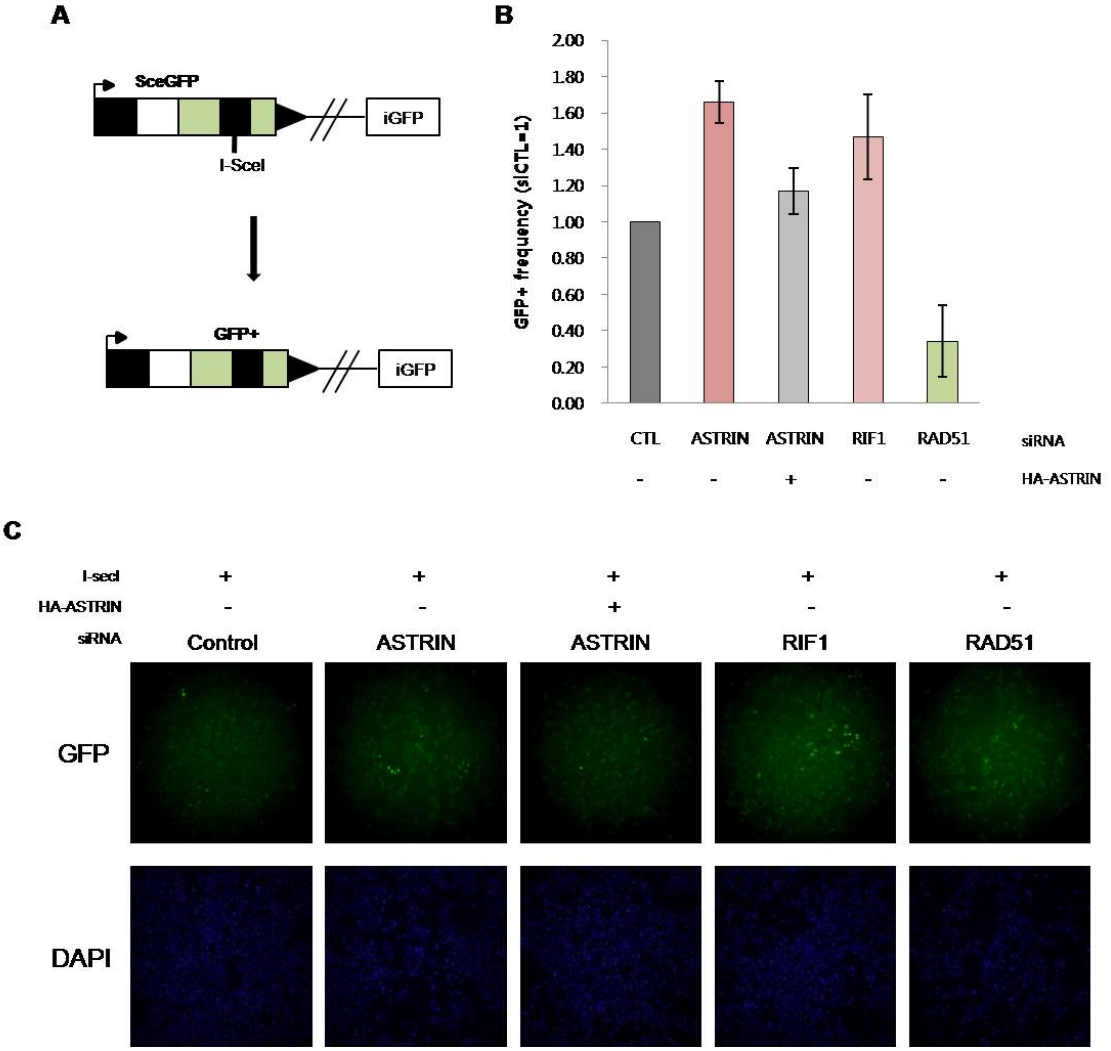

Figure 7. ASTRIN deficiency increases HR.

(A) DR-GFP is shown along with the HDR product that uses iGFP as the tem-plate for nascent DNA synthesis, which results in the restoration of a GFP ex-pression cassette. (B), (C) The efficiency of HR was measured in U2OS cells that contained DR-GFP and had been transfected with control, ASTRIN, RIF1 and RAD51 siRNA for 6 hours and then transfected with an I-SceI expression vector and HA vector or HA-ASTRIN full length. After 48 hours, the population of the GFP-positive cells was measured by IN Cell Analyzer 2500 HS. Quantifi-cation of cells with GFP expression in control, ASTRIN, RIF1, and RAD51 siRNA transfected cells. The % of GFP expressing cells determined. Results are shown as means ±SD (n=3).

8. ASTRIN deficiency increases resection of DSBs.

NHEJ and HR are regulated by DNA end resection steps in the DSB repair, end resection is a characteristic feature of HR. In previous reports, RPA had been formed foci that reflects active resection at the site of DSBs [28, 29]. First, we investigated that RPA foci formation after DSB in G1 phase cells. Control- and ASTRIN-depleted U2OS cells were treated with IR, and then fixed and immunofluorescence assay performed. The cells were co-stained with G2 phase marker, CENP-F. Interestingly, after depletion of ASTRIN, we observed significant increases in the foci formation of RPA in the CENP-F negative cells, G1 cells (Figure 8A and 8B).

RPA foci formation regulates the end resection, and thus we performed 5'-end resection assay using AID DIvA cells. The AsiSI enzyme can be induced to enter the nucleus and generate DSBs at sequence-specific sites (5'-GCGATCGC-3') on treatment of the cells with 4-OHT (Figure 8C). The exten-

sion of 5' end resection, which produces ssDNA at DSB on chromosome was scored by quantitative PCR [26, 30]. As reported, knockdown of CtIP was decreased resection and knockdown of 53BP1 was increased resection. ASTRIN knockdown increased DNA resection by 128%, 115%, and 116% at 364nt, 1754nt, and 3654nt, respectively, from the DSB. 'No DSB' was used as a negative control (Figure 8D). Taken together, we suggested that ASTRIN inhibits the DNA end resection, and therefore decreases the subsequent accumulation of RPA at DSBs in G1 phase of cell cycle.

Figure 8

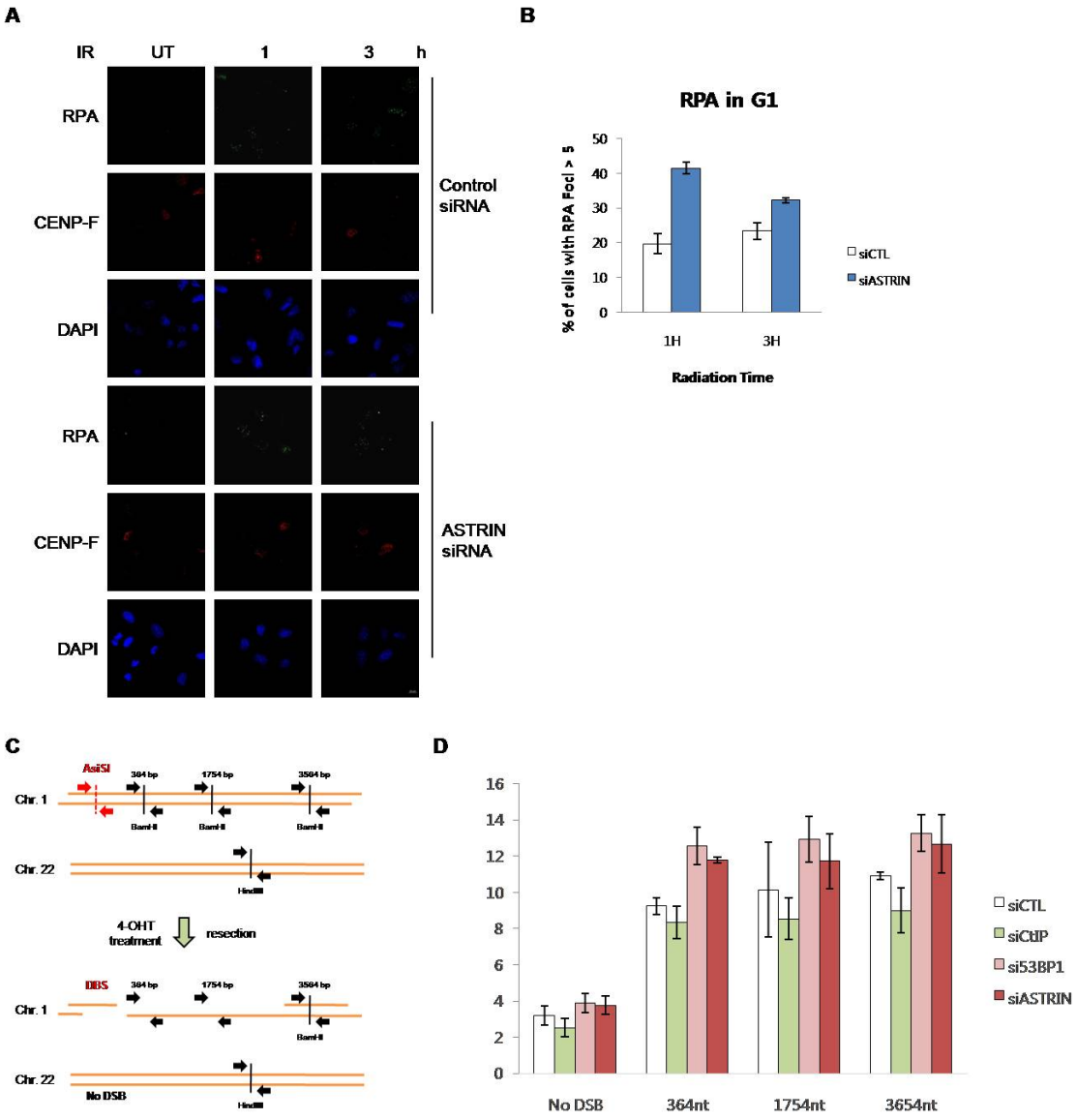

Figure 8. ASTRIN-depleted cells enhance RPA foci formation of DSBs in G1 cells and promote end resection.

(A) Control- and ASTRIN- depleted U2OS cells were untreated or treated with 5 Gy IR and fixed at the indicated times. The cells were stained with an anti-RPA antibody. CENP-F was co-stained with as G2 phase marker. Nuclei were stained with DAPI. (B) Quantification of cells with RPA foci > 5 in the CENP-F negative nuclei. (C) Schematic diagram of ER-AsiSI system. (D) Measurement of DSB resection in AID DIvA cells transfected with control, CtIP, 53BP1, and ASTRIN siRNA. Data are reported as mean ±SD (n=3).

9. ASTRIN is involved in maintaining genome stability.

In previous report, chromosomal aberrations had been increased in RIF1 de-ficiency [31]. So, we hypothesized that depletion of ASTRIN increase chromo-some instability. Control- and ASTRIN- depleted cells treated with 5 Gy IR. After 16 hours, the cells were fixed and metaphase chromosome spreads assay performed. We showed that depletion of ASTRIN was more increase by 50% compared to control cells (Figure 9A and 9B). Because of ASTRIN deficiency, unrepaired damaged cells lead to abnormal chromosomes. Taken together, these results suggest that ASTRIN increases chromosome stability through regulation of DSB repair.

Figure 9

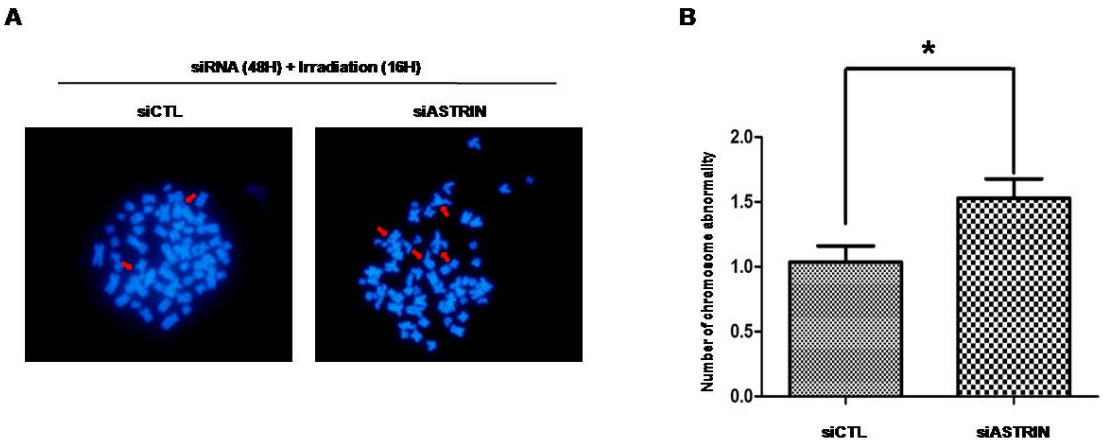

Figure 9. Depletion of ASTRIN increases the number of abnormal chromosomes.

(A) Chromosome instability was induced by depletion of ASTRIN. HeLa cells were treated with control and ASTRIN siRNA and 5 Gy IR before preparation of chromosome spreads. Arrowheads indicate aberrant chromosomes. (B) The numbers of abnormal chromosomes per cell are shown as boxplots. Data are reported as mean ±SD (n=3).

Figure 10

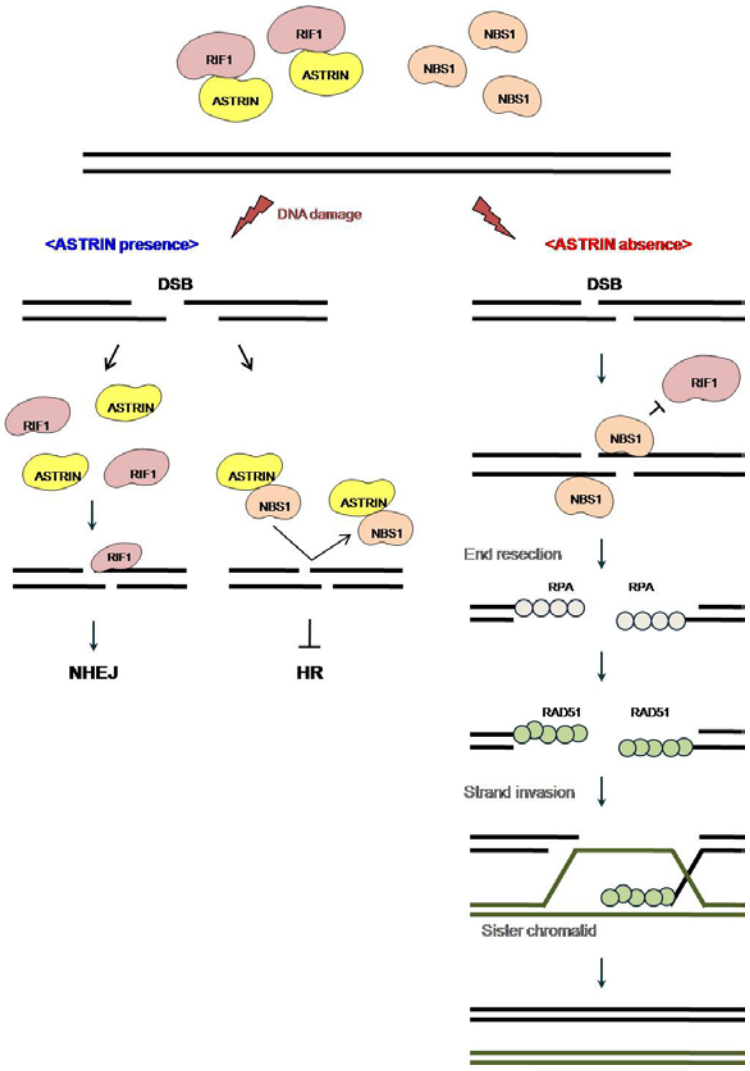

Figure 10. A schematic representation of the role of ASTRIN in regulating the DSB repair is shown.

See Discussion for Details.

DISCUSSION

In this study, we identified that ASTRIN is a novel binding partner of RIF1 and NBS1 by yeast two-hybrid screening, and confirmed by PLA staining and co-immunoprecipitation assay. We revealed that the N-terminal of ASTRIN is essential to RIF1/NBS1 interaction. Depletion of ASTRIN resulted in cellular hypersensitivity and impaired DNA damage repair to IR, as detected by colony survival assay and late γ-H2AX foci staining. Compared with control cells, AS-TRIN-depleted cells decreased IR-induced RIF1 foci but were similar to 53BP1 foci. So, we confirmed that depletion of ASTRIN impaired NHEJ-mediated repair by EJ5-GFP vector system. The contrary, we showed that NBS1 foci, MRE11 foci, RPA foci, RAD51 foci increase in ASTRIN-depleted cells. As well, HR was promoted by depletion of ASTRIN. Moreover, ASTRIN-depleted cells enhanced RPA foci formation in G1 cells and promoted DNA end resection. We finally showed chromosome abnormality in depletion of ASTRIN. In summary, ASTRIN

binds RIF1 and separates NBS1 in untreated condition. But, ASTRIN releases from RIF1 and associates with NBS1 in IR-induced damage. As a result, it promotes NHEJ and inhibits HR. In depletion of ASTRIN, NBS1 recruited at DSBs promotes HR. Thus, our combined results suggest that ASTRIN is a novel regulator of DSB repair choice. The model of ASTRIN function was suggested in Figure 10.

Recent reports are being studied about DNA double-strand break resection. REV7 was reported NHEJ factor by counteracting DNA double-strand break resection [9]. Shieldin is a RIF1 effector complex in DNA double-strand break repair. Shieldin also controls DNA end resection [6]. We identify a novel end resection regulator protein, ASTRIN. We suggest that ASTRIN is RIF1 upstream and 53BP1 downstream because it regulates RIF1 foci but doesn't 53BP1 foci.

However, the exactly contribution of ASTRIN to regulation of end resection is not yet clear. Therefore, we must have done to further demonstrate with de-

tailed mechanism of ASTRIN. We searched for ATM-dependent phosphorylation sites of ASTRIN. ASTRIN has been shown to recognize fifteen phosphor-Ser/Thr motifs. We will investigate to correlation between ASTRIN phosphory-lation and its function using phosphorylation mutants. Moreover, we will investi-gate change of interaction with RIF1 and NBS1 binding partners, such as 53BP1, REV7, Shieldin, CtIP, and MRE11, in the presence or absence of ASTRIN. Fur-ther studies are required to reveal the details of the regulatory mechanisms of ASTRIN in DSB repair pathway choice.

ABSTRACT

ASTRIN mediates RIF1-related DNA damage response

Eun-Bi Yang

Advisor: Prof. Jung-Hee Lee, Ph.D.

Department of Biomedical sciences,

Graduate school of Chosun University

DNA double strand breaks (DSBs) is repaired by two major pathway non-homologous end joining (NHEJ) and homologous recombination (HR). RIF1 promotes non-homologous end joining repair and NBS1 is essential for homologous recombination repair. DSB repair choice is decided by the DNA end resection. However, the molecular mechanism of DNA end resection competition remains elusive. Here, we have identified an ASTRIN as a novel RIF1 and NBS1-binding protein by yeast-two hybrid assay. Interestingly, the ASTRIN increased its binding to NBS1 and decreased its binding to RIF1 after ionizing radiation (IR).

We suggested that ASTRIN had an opposite binding relationship with the NBS1 and RIF1. Depletion of ASTRIN was resulted in cellular hypersensitivity and impaired DNA damage repair to IR, as detected by colony survival assay and late γ-H2AX foci staining. ASTRIN-depleted cells were decreased the RIF1 foci to IR, and increased NBS1, MRE11, RPA and RAD51 damage foci. However, we showed that a 53BP1 damage focus is similar in ASTRIN absence or presence condition. Furthermore, depletion of ASTRIN was shown the decrease of non-homologous end-joining (NHEJ) and the increase of homologous recombination repair (HR). In depletion of ASTRIN, RPA foci formation was increased in G1 and DNA end resection was enhanced. Finally, we showed that a deficiency of ASTRIN lead to chromosomal aberrations by metaphase chromosome spreads assay. Thus, our combined results suggest that ASTRIN is a new player that determines DNA double strand breaks repair pathway.

REFERENCE

1. Aparicio, T., R. Baer, and J. Gautier, *DNA double-strand break repair pathway choice and cancer.* DNA Repair (Amst), 2014. **19**: p. 169-75.
2. Chapman, J.R., M.R. Taylor, and S.J. Boulton, *Playing the end game: DNA double-strand break repair pathway choice.* Mol Cell, 2012. **47**(4): p. 497-510.
3. Lieber, M.R., *The mechanism of double-strand DNA break repair by the nonhomologous DNA end-joining pathway.* Annu Rev Biochem, 2010. **79**: p. 181-211.
4. Escribano-Diaz, C., et al., *A cell cycle-dependent regulatory circuit composed of 53BP1-RIF1 and BRCA1-CtIP controls DNA repair pathway choice.* Mol Cell, 2013. **49**(5): p. 872-83.
5. Ceccaldi, R., B. Rondinelli, and A.D. D'Andrea, *Repair Pathway Choices and Consequences at the Double-Strand Break.* Trends Cell Biol, 2016. **26**(1): p. 52-64.
6. Gupta, R., et al., *DNA Repair Network Analysis Reveals Shieldin as a Key Regulator of NHEJ and PARP Inhibitor Sensitivity.* Cell, 2018. **173**(4): p. 972-988 e23.
7. Chapman, J.R., et al., *RIF1 is essential for 53BP1-dependent nonhomologous end joining and suppression of DNA double-strand break resection.* Mol Cell, 2013. **49**(5): p. 858-71.
8. Boersma, V., et al., *MAD2L2 controls DNA repair at telomeres and DNA breaks by inhibiting 5' end resection.* Nature, 2015. **521**(7553): p. 537-540.
9. Xu, G., et al., *REV7 counteracts DNA double-strand break resection and affects PARP inhibition.* Nature, 2015. **521**(7553): p. 541-544.
10. Karanam, K., et al., *Quantitative live cell imaging reveals a gradual shift between DNA repair mechanisms and a maximal use of HR in mid S phase.* Mol Cell, 2012.

47(2): p. 320-9.

11. Varon, R., et al., *Nibrin, a novel DNA double-strand break repair protein, is mutated in Nijmegen breakage syndrome.* Cell, 1998. **93**(3): p. 467-76.
12. Carney, J.P., et al., *The hMre11/hRad50 protein complex and Nijmegen breakage syndrome: linkage of double-strand break repair to the cellular DNA damage response.* Cell, 1998. **93**(3): p. 477-86.
13. Zhao, S., W. Renthal, and E.Y. Lee, *Functional analysis of FHA and BRCT domains of NBS1 in chromatin association and DNA damage responses.* Nucleic Acids Res, 2002. **30**(22): p. 4815-22.
14. Pardo, B., B. Gomez-Gonzalez, and A. Aguilera, *DNA repair in mammalian cells: DNA double-strand break repair: how to fix a broken relationship.* Cell Mol Life Sci, 2009. **66**(6): p. 1039-56.
15. Falck, J., et al., *CDK targeting of NBS1 promotes DNA-end resection, replication restart and homologous recombination.* EMBO Rep, 2012. **13**(6): p. 561-8.
16. Jimeno, S., et al., *Neddylation inhibits CtIP-mediated resection and regulates DNA double strand break repair pathway choice.* Nucleic Acids Res, 2015. **43**(2): p. 987-99.
17. Liu, H., et al., *The Deubiquitylating Enzyme USP4 Cooperates with CtIP in DNA Double-Strand Break End Resection.* Cell Rep, 2015. **13**(1): p. 93-107.
18. Huertas, P., *DNA resection in eukaryotes: deciding how to fix the break.* Nat Struct Mol Biol, 2010. **17**(1): p. 11-6.
19. Zimmermann, M., et al., *53BP1 regulates DSB repair using Rif1 to control 5' end resection.* Science, 2013. **339**(6120): p. 700-4.
20. Mack, G.J. and D.A. Compton, *Analysis of mitotic microtubule-associated proteins using mass spectrometry identifies astrin, a spindle-associated protein.* Proc Natl

Acad Sci U S A, 2001. **98**(25): p. 14434-9.

21. Yang, Y.C., et al., *Silencing of astrin induces the p53-dependent apoptosis by suppression of HPV18 E6 expression and sensitizes cells to paclitaxel treatment in HeLa cells.* Biochem Biophys Res Commun, 2006. **343**(2): p. 428-34.
22. Cheng, T.S., et al., *hNinein is required for targeting spindle-associated protein Astrin to the centrosome during the S and G2 phases.* Exp Cell Res, 2007. **313**(8): p. 1710-21.
23. Liu, L., et al., *SNM1B/Apollo interacts with astrin and is required for the prophase cell cycle checkpoint.* Cell Cycle, 2009. **8**(4): p. 628-38.
24. Liu, J.Y., et al., *SPAG5 promotes proliferation and suppresses apoptosis in bladder urothelial carcinoma by upregulating Wnt3 via activating the AKT/mTOR pathway and predicts poorer survival.* Oncogene, 2018. **37**(29): p. 3937-3952.
25. Gruber, J., et al., *The mitotic-spindle-associated protein astrin is essential for progression through mitosis.* J Cell Sci, 2002. **115**(Pt 21): p. 4053-9.
26. Lu, H., et al., *RECQL4 Promotes DNA End Resection in Repair of DNA Double-Strand Breaks.* Cell Rep, 2016. **16**(1): p. 161-173.
27. Bennardo, N., et al., *Alternative-NHEJ is a mechanistically distinct pathway of mammalian chromosome break repair.* PLoS Genet, 2008. **4**(6): p. e1000110.
28. Kakarougkas, A., et al., *Co-operation of BRCA1 and POH1 relieves the barriers posed by 53BP1 and RAP80 to resection.* Nucleic Acids Res, 2013. **41**(22): p. 10298-311.
29. Isono, M., et al., *BRCA1 Directs the Repair Pathway to Homologous Recombination by Promoting 53BP1 Dephosphorylation.* Cell Rep, 2017. **18**(2): p. 520-532.
30. Zhou, Y., et al., *Quantitation of DNA double-strand break resection intermediates in human cells.* Nucleic Acids Res, 2014. **42**(3): p. e19.

31. Di Virgilio, M., et al., *Rif1 prevents resection of DNA breaks and promotes immunoglobulin class switching.* Science, 2013. **339**(6120): p. 711-5.